

Steady Non Isothermal Two-Dimensional Flow of Newtonian Fluid in a Stenosed Channel

A. M. Siddiqui^a, T. Haroon^b, A. A. Mirza^{b,*}, A. R. Ansari^c

^a*Department of Mathematics, York Campus, Pennsylvania State University, York, PA 17403, United States*

^b*COMSATS Institute of Information Technology, Park Road, Chak Shahzad, Islamabad, Pakistan*

^c*Department of Mathematics & Natural Sciences, Gulf University for Science & Technology, P.O. Box 7207, Hawally 32093, Kuwait*

Abstract

In this paper, the steady two-dimensional motion of an incompressible Newtonian fluid between two parallel plates with heat transfer in the presence of a cosine shaped stenosis is studied. The governing equations are transformed into a compatibility and energy equations, which is solved analytically with the help of the regular perturbation technique. The solutions obtained from the present analysis are given in terms of streamlines, wall shear stress, separation and reattachment points, pressure and temperature distributions through the stenosed channel. The accuracy of the results are verified from available literature. It is found that the wall shear stress, pressure gradient and temperature increase with the development of the stenosis, causing separation and reattachment points in the region. It is also observed that even at low velocity, separation occurs if the thickness of the stenosis is increased. We present the results in graphical form.

Keywords: Newtonian fluid, stenosis, heat transfer.

2010 MSC: 76-XX.

1. Introduction

The motivation of this study comes from the investigation of abnormal blood flow in a stenosed artery, which may be due to atherosclerotic plaques developed at various locations in the artery. Its effect on the flow of blood is discussed by many authors theoretically, experimentally as well as numerically. Forrester and Young (Forrester & Young, 1970) presented the theoretical as well as experimental results of an axisymmetric, steady flow through a converging and diverging tube with mild stenosis. It is observed that there is an abundant amount of evidence to support the conclusion that the abnormal flow conditions developed in a stenotic obstruction can be an important

*Corresponding author

Email address: azharali_mirza1@yahoo.com (A. A. Mirza)

factor in the development and progression of arterial disease. Further indicate that even a mild collarlike stenosis in a small artery can create significant abnormalities in the flow. Morgan and Young (Morgan & Young, 1974) provided the approximate analytical solution of axisymmetric, steady flow of incompressible Newtonian fluid both for mild and severe stenosis by using an integral method; basically they presented the extension of Forrester (Forrester & Young, 1970). It is observed that even a mild stenosis can cause a radical alteration in flow characteristics and that the effect in general becomes more drastic as the stenosis becomes more severe and the Reynolds number increases and also wall shearing stress is especially affected. Analysis of blood flow using an incompressible Newtonian fluid through an axisymmetric stenosed artery of cosine shape has been done by K. Haldar (Haldar, 1991). It is shown that for any given Reynolds number or tube constriction the separation point moves towards the throat of the tube and the reattachment point moves downstream with the enlargement of the region of separation which is physiologically unfavorable. Layek and Midya (Layek & Midya, 2007) presented the numerical solution of a time dependent incompressible Newtonian fluid for symmetric stenosis in a two dimensional channel. It is noticed that the maximum stress and the length of the recirculating region associated with two shear layers of the constriction increase with the increase of the area reduction of the constriction. It is observed that the critical values for three constriction heights $h = 0.25, 0.3, 0.35$ are 600, 300, 210 respectively. Chow et al. (Chow et al., 1971) analyzed the steady laminar flow of an incompressible Newtonian fluid for different physical parameters by considering a sinusoidal boundary. It is observed that by increasing either Re or ϵ , the separation point would move down towards the throat in the divergent part of the channel with subsequent enlargement of the region of separation. Lee and Fung (Lee & Fung, 1970) solved the flow model of the Newtonian fluid numerically through locally constricted tube for the low Reynolds number. The constraints in their numerical procedure restricted the shape of the tube to be fixed and the Reynolds number to be moderate. Haldar (Haldar, 1985) discussed the effect of the shape of constriction on the resistance of blood flow through an artery with mild local narrowing. It is shown that the resistance to flow decreases as the shape of the stenosis changes and maximum resistance is attained for symmetric stenosis. S. Chakravarty and A. Ghosh Chakravarty (Chakravarty & Chakravarty, 1988) presented analytical solutions by considering an anisotropically elastic cylindrical tube filled with viscous incompressible fluid representing blood having stenosis. The analysis is carried out for an artery with mild local narrowing in its lumen forming a stenosis. K. Haldar (Kruszewski et al., 2008) studied the oscillatory flow of blood which behaves as a Newtonian fluid having surface roughness of cosine shape. It is observed that the resistive impedance and wall shear stress increases as the phase lag increases for a particular value of stenosis height. It is also observed that impedance and wall shear stress increases with the increase in the stenosis height. Newman et al. (Newman et al., 1979) investigated the oscillatory flow numerically in a rigid tube with stenosis. The predictions of the numerical results agreed well with the experimental works. This paper deals with the problem of oscillatory blood flow through a rigid tube with a mild constriction under a simple-harmonic pressure gradient examines the effect of stenosis on the flow field by considering blood as a Newtonian fluid. Mehrotra et al. (Mehrotra et al., 1985) presented analysis by considering the flow in a stenotic tube where the cross-section is elliptic. It is observed that the theoretical study of pulsatile flow in a stenotic tube confirms the view that the fluid dynamics characteristics of the flow are affected by the percentage of stenosis as well as the geometry of the stenosis. The

frequency of oscillation also influences the shearing stress. Srivastava and Rastogi (Srivastava & Rastogi, 2010) investigated the blood flow through narrow catheterized artery with an axially nonsymmetrical stenosis. It is found that the flow resistance increases with the catheter size, the hematocrit and the stenosis size but decreases with the shape parameter. A significant increase in the magnitude of the impedance and the wall shear stress occurs even for a small increase in the catheter size. The shear stress at the stenosis throat decreases with the increasing catheter size. The abnormal flow conditions developed due to stenosis can be an important factor in the development and progression of arterial diseases. Some of the further major complications developed through these stenosis are the growth of tissues into arteries, development of an intravascular clot and post-stenotic dilatation. This type of flow also has applications in various fields like physiological flows and polymer science.

In the present paper, the effect of stenosis height and Reynolds number on flow characteristics, wall shear stress, pressure gradient, separation and reattachment points and heat transfer are analyzed. The study of the Peclet number and Brinkman number on the temperature distribution is also presented. It is observed that the general pattern of flow is similar to the results given in (Haldar, 1991) - (Chow et al., 1971). The results of the present investigation indicate that even a mild collar like stenosis in a small artery can create significant abnormalities in the flow including the phenomenon of separation. This study presents the steady, two-dimensional motion of an incompressible Newtonian fluid in a cosine shaped stenosed channel with heat transfer. In this analysis blood is assumed as Newtonian fluid and the geometry of the artery is approximated by a channel. The layout of the paper is as follows: The basic equations governing the flow, in the Cartesian coordinate, are given in section 2. Problem formulation is presented in Section 3. In Section 4 the method is discussed and section 5 is dedicated the solution for different parameters. Section 6 provides a graphical discussion. A summary is given in section 7.

2. Governing equations

The basic governing equations for steady two dimensional flow of a non-isothermal, incompressible linearly viscous fluid in the absence of body forces are

$$\widetilde{\nabla} \cdot \widetilde{\mathbf{V}} = 0, \quad (2.1)$$

$$\rho \frac{d\widetilde{\mathbf{V}}}{dt} = -\widetilde{\nabla} \widetilde{p} + \widetilde{\nabla} \widetilde{\tau}, \quad (2.2)$$

$$\rho c_p \frac{d\widetilde{T}}{dt} = \kappa \widetilde{\nabla}^2 \widetilde{T} + \phi, \quad (2.3)$$

where $\widetilde{\mathbf{V}}$, \widetilde{T} and ρ are the velocity vector, temperature and constant density of the fluid respectively, \widetilde{p} is the dynamic pressure, c_p and κ are the specific heat and thermal conductivity parameters respectively, $\widetilde{\nabla}^2$ is the Laplacian, ϕ the viscous dissipation function defined as $\phi = \widetilde{\tau} \cdot \widetilde{\nabla} \widetilde{\mathbf{V}}$ and d/dt the material time derivative defined as

$$\frac{d}{dt} = \frac{\partial}{\partial t} + \widetilde{u} \frac{\partial}{\partial x} + \widetilde{v} \frac{\partial}{\partial y}, \quad (2.4)$$

where \bar{u} and \bar{v} are the velocity components in \bar{x} and \bar{y} directions, respectively and $\bar{\tau}$ is the extra stress tensor defined as follows

$$\bar{\tau} = \mu \bar{\mathbf{A}}_1, \quad (2.5)$$

where μ is the dynamic viscosity and \mathbf{A}_1 the first Rivlin-Ericksen tensor defined as

$$\bar{\mathbf{A}}_1 = \bar{\nabla} \bar{\mathbf{V}} + (\bar{\nabla} \bar{\mathbf{V}})^{\top}, \quad (2.6)$$

here \top indicates the transpose.

3. Problem formulation

Consider the non-isothermal Newtonian flow through the channel of infinite length with heat transfer having stenosis of length $l_o/2$. The coordinate system is chosen in such a way that the arterial system lies in the $\bar{x}\bar{y}$ -plane, such that \bar{x} -axis coincide with the center line in the direction of flow and \bar{y} -axis perpendicular to \bar{x} -axis.

Consider the boundary of the stenosed region of the form (Haldar, 1991)

$$\begin{aligned} h(\bar{x}) &= h_o - \frac{\lambda}{2} \left(1 + \cos \left(\frac{4\pi\bar{x}}{l_o} \right) \right) \quad -\frac{l_o}{4} < \bar{x} < \frac{l_o}{4}, \\ &= h_o \quad \text{otherwise,} \end{aligned} \quad (3.1)$$

where $h(\bar{x})$ is variable gap between the stenosis, $2h_o$ the width of unobstructed channel and λ the maximum height of stenosis.

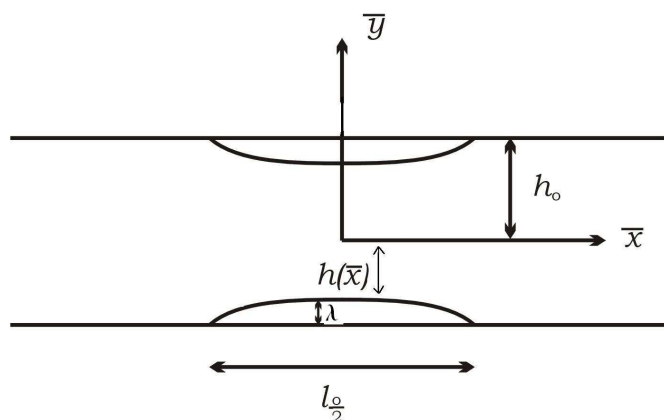


Figure 1. Geometry of the problem.

Boundary conditions for the present problem are

$$\begin{aligned} \bar{u} &= \bar{v} = 0, \quad \bar{T} = T_1 \quad \text{at} \quad \bar{y} = h(\bar{x}), \\ \frac{\partial \bar{u}}{\partial \bar{y}} &= 0, \quad \frac{\partial \bar{T}}{\partial \bar{y}} = 0 \quad \text{at} \quad \bar{y} = 0, \\ \bar{Q} &= 2 \int_0^{h(\bar{x})} \bar{u} d\bar{y} = -u_o h_o, \end{aligned} \quad (3.2)$$

where u_o is the average velocity and \bar{Q} the volume flow rate. Assume that the blood behaves like Newtonian fluid and for steady, homogeneous, incompressible two dimensional flow of blood velocity field is assumed as

$$\bar{\mathbf{V}} = (\bar{u}(\bar{x}, \bar{y}), \bar{v}(\bar{x}, \bar{y}), 0). \quad (3.3)$$

Introducing the dimensionless parameters as follows

$$u = \frac{\bar{u}}{u_o}, \quad v = \frac{\bar{v}}{u_o}, \quad x = \frac{\bar{x}}{l_o}, \quad y = \frac{\bar{y}}{h_o}, \quad p = \frac{h_o^2}{\mu u_o l_o} \bar{p}, \quad \theta = \frac{\bar{T} - T_o}{T_1 - T_o}, \quad (3.4)$$

where T_1 and T_o are temperatures on the boundary of stenosis and fluid respectively.

Substituting equations (2.4)-(2.6) in equations (2.1) - (2.3) and making use of (3.3) and (3.4), nondimensional form of equations becomes

$$\delta \frac{\partial u}{\partial x} + \frac{\partial v}{\partial y} = 0, \quad (3.5)$$

$$Re \left(\delta u \frac{\partial u}{\partial x} + v \frac{\partial u}{\partial y} \right) = -\frac{\partial p}{\partial x} + \nabla^2 u, \quad (3.6)$$

$$Re \delta \left(\delta u \frac{\partial v}{\partial x} + v \frac{\partial v}{\partial y} \right) = -\frac{\partial p}{\partial y} + \delta \nabla^2 v, \quad (3.7)$$

$$Pe \left(\delta u \frac{\partial \theta}{\partial x} + v \frac{\partial \theta}{\partial y} \right) = \nabla^2 \theta + Br \left(4\delta^2 \left(\frac{\partial u}{\partial x} \right)^2 + \left(\frac{\partial u}{\partial y} + \delta \frac{\partial v}{\partial x} \right)^2 \right), \quad (3.8)$$

where

$$\delta = \frac{h_o}{l_o}, \quad Re = \frac{u_o h_o}{\nu}, \quad Br = \frac{\mu u_o^2}{\kappa(T_1 - T_o)}, \quad Pe = \frac{\rho c_p h_o u_o}{\kappa}, \quad (3.9)$$

in which Re is the Reynolds number, Br the Brinkman number, Pe the Peclet number.

Now to convert these equations in single variable, introducing the stream function defined as

$$u = \frac{\partial \psi}{\partial y}, \quad v = -\delta \frac{\partial \psi}{\partial x}, \quad (3.10)$$

which satisfy the continuity equation (3.5) identically. After eliminating pressure gradient term from momentum equations (3.6)-(3.7) and making use of (3.10), compatibility equation is obtained of the form

$$Re \delta \frac{\partial (\psi, \nabla^2 \psi)}{\partial (y, x)} = \nabla^4 \psi, \quad (3.11)$$

where $\nabla^2 = \delta^2 \frac{\partial^2}{\partial x^2} + \frac{\partial^2}{\partial y^2}$, is the dimensionless form of the Laplacian. Energy equation (3.8) in terms of stream function becomes

$$Pe \delta \frac{\partial (\psi, \theta)}{\partial (y, x)} = \nabla^2 \theta + Br \left(4\delta^2 \left(\frac{\partial^2 \psi}{\partial x \partial y} \right)^2 + \left(\frac{\partial^2 \psi}{\partial y^2} - \delta^2 \frac{\partial^2 \psi}{\partial x^2} \right)^2 \right). \quad (3.12)$$

The dimensionless stenosis profile (3.1) takes the form

$$\begin{aligned} f(x) &= 1 - \frac{\epsilon}{2}(1 + \cos 4\pi x) & -\frac{1}{4} < x < \frac{1}{4}, \\ &= 1 & \text{otherwise,} \end{aligned} \quad (3.13)$$

where $f = \frac{h(\bar{x})}{h_o}$ and $\epsilon = \frac{\lambda}{h_o}$.

Boundary conditions in terms of stream function becomes

$$\begin{aligned} \frac{\partial \psi}{\partial y} &= 0, \quad \psi = -\frac{1}{2}, \quad \theta = 1 \quad \text{at} \quad y = f, \\ \frac{\partial^2 \psi}{\partial y^2} &= 0, \quad \psi = 0, \quad \frac{\partial \theta}{\partial y} = 0 \quad \text{at} \quad y = 0. \end{aligned} \quad (3.14)$$

Due to non-linearity of (3.11) and (3.12), the regular perturbation technique is applied to find the analytical solution along with the boundary conditions defined in (3.14).

4. Perturbation method

In this section we shall discuss the perturbation method by considering a linear or nonlinear differential equation

$$L(\psi, \delta) = 0, \quad (4.1)$$

that depends on the small positive parameter δ . The boundary or initial conditions may depend on δ . The reduced or unperturbed problem associated with the problem is obtained by setting $\delta = 0$ along with its boundary or initial conditions. We expand the solution ψ in the perturbation series

$$\psi = \sum_{n=0}^{\infty} \psi_n \delta^n, \quad (4.2)$$

the difference between ψ and ψ_o is referred to as a perturbation on the solution ψ_o of the reduced problem. Inserting this equation into (4.1) gives

$$L(\psi, \delta) = L\left(\sum_{n=0}^{\infty} \psi_n \delta^n, \delta\right) = 0. \quad (4.3)$$

We assume that $L(\psi, \delta)$ can be expanded in a power series in ψ and δ . As a result above equation (4.3) can be expanded in the form of the series

$$L(\psi, \delta) = \sum_{n=0}^{\infty} L_n(\psi_n, \psi_{n-1}, \dots, \psi_1, \psi_o) \delta^n = 0, \quad (4.4)$$

where L_n represents differential operator, which may be linear or nonlinear. The series (4.2) is also inserted into the given initial and boundary conditions for the problem.

To solve the given problem by means of the perturbation method, we put the coefficient of δ^n in (4.4) equal to zero and obtain

$$L_n(\psi_n, \psi_{n-1}, \dots, \psi_1, \psi_o) = 0, n = 0, 1, 2, \dots. \quad (4.5)$$

Similarly we equate coefficient of like powers of δ in the initial or boundary conditions. This yields the system of equations (4.5) with appropriate boundary conditions that we solve recursively.

We first solve the reduced equation

$$L_o(\psi_o) = 0, \quad (4.6)$$

with relevant boundary conditions. Once ψ_o is found, then equation for ψ_1 with boundary conditions is

$$L_1(\psi_1, \psi_o) = 0, \quad (4.7)$$

is solved and then the equations for ψ_2, ψ_3, \dots with relevant boundary or initial conditions are solved successively.

5. Solution

To solve the compatibility equation and energy equation along with boundary conditions (3.14), the flow variables ψ and θ are perturbed as

$$\begin{aligned} \psi &= \psi_o + \delta\psi_1 + \delta^2\psi_2 + \dots, \\ \theta &= \theta_o + \delta\theta_1 + \delta^2\theta_2 + \dots. \end{aligned} \quad (5.1)$$

where δ is a small parameter.

5.1. Zeroth order problem and its solution

Zeroth order system of equations is obtained by substituting (5.1) in equations (3.11)-(3.12), (3.14) and equating the coefficients of δ^0 as

$$\frac{\partial^4 \psi_o}{\partial y^4} = 0, \quad (5.2)$$

$$\frac{\partial^2 \theta_o}{\partial y^2} = -Br \left(\frac{\partial^2 \psi_o}{\partial y^2} \right)^2, \quad (5.3)$$

and corresponding boundary conditions

$$\begin{aligned} \frac{\partial \psi_o}{\partial y} = 0, \quad \psi_o = -\frac{1}{2}, \quad \theta_o = 1 \quad \text{at} \quad y = f, \\ \frac{\partial^2 \psi_o}{\partial y^2} = 0, \quad \psi_o = 0, \quad \frac{\partial \theta_o}{\partial y} = 0 \quad \text{at} \quad y = 0. \end{aligned} \quad (5.4)$$

The solution of equation (5.2) along with boundary conditions (5.4) is given of the form

$$\psi_o = \frac{\eta}{4} (\eta^2 - 3), \quad \text{where} \quad \eta = \frac{y}{f}. \quad (5.5)$$

After substitution of (5.5) in (5.3) subject to (5.4), zeroth order temperature is obtained as

$$\theta_o = 1 - \frac{3Br}{16f^2} (\eta^4 - 1), \quad (5.6)$$

which indicates that the temperature depends upon the ratio of heat production by viscous dissipation to heat transport by conduction.

5.2. First order problem and its solution

For the first order system comparing the coefficients of δ , we get

$$\frac{\partial^4 \psi_1}{\partial y^4} = Re \frac{\partial \left(\psi_o, \frac{\partial^2 \psi_o}{\partial y^2} \right)}{\partial (y, x)}, \quad (5.7)$$

$$\frac{\partial^2 \theta_1}{\partial y^2} = Pe \frac{\partial (\psi_o, \theta_o)}{\partial (y, x)} - 2Br \left(\frac{\partial^2 \psi_o}{\partial y^2} \frac{\partial^2 \psi_1}{\partial y^2} \right), \quad (5.8)$$

and boundary conditions

$$\begin{aligned} \frac{\partial \psi_1}{\partial y} = 0, \quad \psi_1 = 0 \quad \theta_1 = 0 \quad \text{at} \quad y = f, \\ \frac{\partial^2 \psi_1}{\partial y^2} = 0, \quad \psi_1 = 0, \quad \frac{\partial \theta_1}{\partial y} = 0 \quad \text{at} \quad y = 0. \end{aligned} \quad (5.9)$$

The solution of equation (5.7) by making use (5.5) and (5.9) becomes

$$\psi_1 = -\frac{3Ref'\eta}{1120} (\eta^6 - 7\eta^4 + 11\eta^2 - 5). \quad (5.10)$$

By substitution of (5.5) and (5.10) in equation (5.8) and making use of (5.9), the first order temperature profile is obtained of the form

$$\theta_1 = \frac{3Brf'(\eta^2 - 1)}{8960f^2} \left\{ 2Re(9\eta^6 - 47\eta^4 + 19\eta^2 + 19) + Pe(15\eta^6 - 13\eta^4 - 83\eta^2 + 337) \right\}. \quad (5.11)$$

It is observed that the first order temperature depends upon the ratio of heat production by viscous dissipation and heat transport by convection to heat transport by conduction.

5.3. Second order problem and its solution

Comparing the coefficients of δ^2 to get the second order system as

$$\frac{\partial^4 \psi_2}{\partial y^4} = Re \left[\frac{\partial \left(\psi_o, \frac{\partial^2 \psi_1}{\partial y^2} \right)}{\partial (y, x)} + \frac{\partial \left(\psi_1, \frac{\partial^2 \psi_o}{\partial y^2} \right)}{\partial (y, x)} \right] - 2 \frac{\partial^4 \psi_o}{\partial x^2 \partial y^2}, \quad (5.12)$$

$$\begin{aligned} \frac{\partial^2 \theta_2}{\partial y^2} = & Pe \left[\frac{\partial(\psi_o, \theta_1)}{\partial(y, x)} + \frac{\partial(\psi_1, \theta_o)}{\partial(y, x)} \right] - \frac{\partial^2 \theta_o}{\partial x^2} - Br \left[4 \left(\frac{\partial^2 \psi_o}{\partial x \partial y} \right)^2 + \left(\frac{\partial^2 \psi_1}{\partial y^2} \right)^2 \right. \\ & \left. + 2 \frac{\partial^2 \psi_o}{\partial y^2} \frac{\partial^2 \psi_2}{\partial y^2} - 2 \frac{\partial^2 \psi_o}{\partial y^2} \frac{\partial^2 \psi_o}{\partial x^2} \right], \end{aligned} \quad (5.13)$$

boundary conditions for second order system are

$$\begin{aligned} \frac{\partial \psi_2}{\partial y} = 0, \quad \psi_2 = 0, \quad \theta_2 = 0 \quad \text{at} \quad y = f, \\ \frac{\partial^2 \psi_2}{\partial y^2} = 0, \quad \psi_2 = 0, \quad \frac{\partial \theta_2}{\partial y} = 0 \quad \text{at} \quad y = 0. \end{aligned} \quad (5.14)$$

Using (5.5) and (5.10) in equation (5.12), the solution is obtained by successive integration along with the boundary conditions defined in (5.14) as follows

$$\begin{aligned} \psi_2 = & CRe^2 \eta \left[f'^2 (98\eta^{10} - 1155\eta^8 + 4488\eta^6 - 8778\eta^4 + 8222\eta^2 - 2875) \right. \\ & \left. - f f'' (35\eta^{10} - 385\eta^8 + 1518\eta^6 - 3234\eta^4 + 3279\eta^2 - 1213) \right] - \frac{3\eta(4f'^2 - f f'')}{40} (\eta^4 - 2\eta^2 = 1), \end{aligned} \quad (5.15)$$

which is second order solution for stream lines. To find the second order temperature, using (5.5), (5.10) and (5.15) in equation (5.13), with the help of MATHEMATICA, we get

$$\begin{aligned} \theta_2 = & \frac{C_1(\eta^2 - 1)}{f^2} \left[-4f'^2 \left\{ 7Pe^2 (225\eta^{10} - 721\eta^8 - 220\eta^6 + 30134\eta^4 - 94771\eta^2 + 238859) \right. \right. \\ & + 2PeRe (840\eta^{10} - 6860\eta^8 + 11455\eta^6 + 3139\eta^4 - 26891\eta^2 + 56269) + Re^2 (2303\eta^{10} \\ & - 21721\eta^8 + 63122\eta^6 - 68086\eta^4 + 17183\eta^2 + 17183) - 517440(13\eta^4 + 9\eta^2 - 36) \left. \right\} \\ & + f f'' \left\{ 3Br \left(7Pe^2 (225\eta^{10} - 721\eta^8 - 2206\eta^6 + 30134\eta^4 - 94771\eta^2 + 238859) \right. \right. \\ & + 2PeRe (525\eta^{10} - 5173\eta^8 + 14132\eta^6 - 7120\eta^4 - 29065\eta^2 + 102605) + 8Re^2 (175\eta^{10} \\ & - 1673\eta^8 + 5158\eta^6 - 7778\eta^4 + 2059\eta^2 + 2059) - 2069760(7\eta^4 - 4\eta^2 - 9) \left. \right\} \left. \right]. \end{aligned} \quad (5.16)$$

5.4. Velocity and temperature fields

The dimensionless velocity components in x and y directions are obtained from (3.10), we arrive at the axial component of velocity as

$$\begin{aligned} u = & \frac{(\eta^2 - 1)}{f} \left[\frac{3}{4} - \frac{3Re\delta f'}{1120} (7\eta^4 - 28\eta^2 + 5) + \delta^2 \left\{ \frac{3}{40} (f f'' - 4f'^2) (5\eta^2 - 1) \right. \right. \\ & + CRe^2 \left\{ f'^2 (1078\eta^8 - 9317\eta^6 + 22099\eta^4 - 21791\eta^2 + 2875) \right. \\ & \left. \left. - C f f'' (385\eta^8 - 3080\eta^6 + 7546\eta^4 - 8624\eta^2 + 1213) \right\} \right], \end{aligned} \quad (5.17)$$

and the normal component of velocity is

$$v = \frac{\delta\eta(\eta^2 - 1)}{f} \left[\frac{3}{4}f' + \frac{3Re\delta}{20} (ff''(\eta^2 - 1)(\eta^2 - 5) - f'^2(7\eta^4 - 28\eta^2 + 5)) \right. \\ \left. + \delta^2 \left\{ \frac{3ff'f''}{10} (3\eta^2 - 1) - \frac{3f^2f''}{40} (\eta^2 - 1) - \frac{3f'^3}{10} (5\eta^2 - 1) + Re^2 \{ Cf'^3 (1078\eta^8 \right. \quad (5.18) \\ \left. - 93172\eta^6 + 22099\eta^4 - 21791\eta^2 + 28875) - C_2ff'f'' (273\eta^8 - 2422\eta^6 + 6620\eta^4 \right. \\ \left. - 8626\eta^2 + 2875) + Cf^2f'' (\eta^2 - 1) (35\eta^6 - 315\eta^4 + 853\eta^2 - 1213) \} \right\} \right].$$

The temperature distribution up to second order is obtained from (5.1), we arrive

$$\theta = 1 - \frac{Br}{f^2} \left[\frac{3}{16}(\eta^4 - 1) - \delta \left\{ \frac{3f'(\eta^2 - 1)}{8960} (2Re(9\eta^6 - 47\eta^4 + 19\eta^2 + 19) + Pe(15\eta^6 - 13\eta^4 \right. \right. \\ \left. \left. - 83\eta^2 + 337)) \right\} - \delta^2 \left[C_1(\eta^2 - 1) \{ -2f'^2 \{ 7Pe^2(225\eta^{10} - 721\eta^8 - 2206\eta^6 + 30134\eta^4 \right. \right. \\ \left. \left. - 94771\eta^2 + 238859) + 4PeRe(840\eta^{10} - 6860\eta^8 + 11455\eta^6 + 3139\eta^4 - 26891\eta^2 + 56269) \right. \right. \\ \left. \left. + 2Re^2(2303\eta^{10} - 21721\eta^8 + 63122\eta^6 - 68086\eta^4 + 17183\eta^2 + 17183) - 1034880(13\eta^4 \right. \right. \\ \left. \left. + 9\eta^2 - 36) \} \right\} + ff'' \{ 3Br \{ 7Pe^2(225\eta^{10} - 721\eta^8 - 2206\eta^6 + 30134\eta^4 - 94771\eta^2 + 238859) \right. \\ \left. \left. + 2PeRe(525\eta^{10} - 5173\eta^8 + 14132\eta^6 - 7120\eta^4 - 29065\eta^2 + 102605) + 8Re^2(175\eta^{10} - 1673\eta^8 \right. \right. \\ \left. \left. + 5158\eta^6 - 7778\eta^4 + 2059\eta^2 + 2059) - 2069760(7\eta^4 - 4\eta^2 - 9) \} \} \right] \right], \quad (5.19)$$

where $C = \frac{1}{3449600}$, $C_1 = \frac{1}{55193600}$, $C_2 = \frac{1}{1724800}$. Dimensionless wall shear stress for viscous fluid up to second order is given by

$$\tau_\omega = \left(\frac{\partial u}{\partial y} + \delta \frac{\partial v}{\partial x} \right)_{y=f} \\ = \frac{3}{f^2} \left[\frac{1}{2} + \frac{Ref'}{35} \delta + \frac{\delta^2}{10} \left\{ \frac{Re^2}{8085} (40ff'' - 79f'^2) + (2ff'' - 13f'^2) \right\} \right]. \quad (5.20)$$

The points of separation and reattachment are defined as the back flow at wall, where the wall shear stress is zero, i.e. $\tau_\omega = 0$, then above equation reduces as

$$40425 + 2310Ref'\delta + \delta^2 \{ 10ff'' (40Re^2 + 16170) - f'^2 (79Re^2 + 105105) \} = 0. \quad (5.21)$$

The solution of (5.21) in terms of Reynolds number Re is

$$Re = \frac{7}{\delta(40ff'' - 79f'^2)} \left\{ -165f' \pm \sqrt{165 \{ 165f'^2 - (40ff'' - 79f'^2)(5 - 13\delta^2f'^2 + 2\delta^2ff'') \}} \right\}. \quad (5.22)$$

By using equation (5.22), our aim is to find graphically the critical Reynolds number at which the back flow occur.

5.5. Pressure distribution

To find the pressure distribution along x-axis within the channel, the equations (3.6) and (3.7) are converted in terms of stream function and then perturb these equation by using (5.1) and

$$p = p_o + \delta p_1 + \delta^2 p_2 + \cdots, \quad (5.23)$$

system of equations is obtained as follows.

5.5.1. Zeroth order pressure and solution

Comparing the coefficients of δ^0 , we get

$$\frac{\partial p_o}{\partial x} = \frac{\partial^3 \psi_o}{\partial y^3}, \quad (5.24)$$

$$\frac{\partial p_o}{\partial y} = 0. \quad (5.25)$$

By integrating the above two equations and making use of (5.5), the zeroth order pressure is obtained of the form

$$p_o = \frac{3}{32\pi(\epsilon - 1)^2} \left[\frac{1}{\sqrt{1 - \epsilon}} (3\epsilon^2 - 8\epsilon + 8) \tan^{-1} \left(\frac{\tan 2\pi x}{\sqrt{1 - \epsilon}} \right) - \frac{f'}{8\pi f^2} \{ 16(\epsilon - 1) - 3\epsilon^2 - 3\epsilon(\epsilon - 2) \cos(4\pi x) \} \right], \quad (5.26)$$

which involves the trigonometric and inverse trigonometric function.

5.5.2. First order pressure and solution

Equating the coefficients of δ , we obtain

$$\frac{\partial p_1}{\partial x} = \frac{\partial^3 \psi_1}{\partial y^3} - Re \frac{\partial \left(\psi_o, \frac{\partial \psi_o}{\partial y} \right)}{\partial (y, x)}, \quad (5.27)$$

$$\frac{\partial p_1}{\partial y} = 0, \quad (5.28)$$

by making use of equations (5.5), (5.10) and solving (5.27)-(5.28), the first order solution for pressure is obtained by applying

$$p_1 = \int_0^x \frac{\partial p_1}{\partial x} dx + \int_0^y \frac{\partial p_1}{\partial y} dy, \quad (5.29)$$

of the form

$$p_1 = \frac{27Re}{140f^2} \left(\frac{1}{(1 - \epsilon)^2} - \frac{1}{f^2} \right). \quad (5.30)$$

5.5.3. Second order pressure and solution

Comparing the coefficients of δ^2 , we arrive at

$$\frac{\partial p_2}{\partial x} = \frac{\partial^3 \psi_2}{\partial y^3} - Re \left[\frac{\partial \left(\psi_o, \frac{\partial \psi_1}{\partial y} \right)}{\partial (y, x)} + \frac{\partial \left(\psi_1, \frac{\partial \psi_o}{\partial y} \right)}{\partial (y, x)} \right], \quad (5.31)$$

$$\frac{\partial p_2}{\partial y} = -\frac{\partial^3 \psi_o}{\partial x \partial y^2}, \quad (5.32)$$

by integrating the equations (5.31)-(5.32) and making use of (5.5), (5.10) and (5.15), we arrive at the second order pressure as follows

$$p_2 = \frac{3}{13475} \left[\frac{\pi \epsilon^2}{(1 - \epsilon)^{\frac{3}{2}}} (13Re^2 + 8085) \tan^{-1} \left(\frac{\tan 2\pi x}{\sqrt{1 - \epsilon}} \right) + f' \left\{ \frac{40425\eta^2}{2f^2} + \frac{52Re^2 - 18865}{4f^2} + \frac{(\epsilon - 2)(13Re^2 + 8085)}{4f(\epsilon - 1)} \right\} \right]. \quad (5.33)$$

Now one can easily find the pressure up to second order by using equations (5.26), (5.30) and (5.33).

6. Graphical discussion

In this section the effect of different pertinent parameters on stream lines, wall shear stress, pressure distribution, separation and reattachment points and analysis for heat transfer are presented graphically. The geometry of the proposed model for the study of the stenosed artery is depicted in Figure 1. The radii of obstructed and unobstructed regions are $h(x)$ and h_o . The point of separation lies near the throat of the stenosed region in the converging section. Separation point means the point where reverse flow occurs. Figure 2,3 presents the behavior of stream lines for zeroth order in 2(a), first order in 2(b), second order in 3(a) and up to second order in 3(b) respectively, for the fixed values of $Re = 12$, $\epsilon = 0.2$, $\delta = 0.1$, $\alpha = 0.04$. In these figures x - axis lies in the horizontal direction and y - axis perpendicular to it. The zeroth order solution corresponds to the flow with vanishing wall slopes and reduces to the flow between parallel plates for $\epsilon = 0$. The stream lines are relatively straight in the center of the channel. The first order solution induces the clockwise and counterclockwise rotational motion in the converging and diverging regions, which indicates the separation point in the converging region and reattachment point in the diverging region. Figure 3(a) shows the stream lines for second order solution reinforce the first order solution and observe the rotational motion which predicts the separation and reattachment points. Figure 3(b) presents the stream lines up to second order. It is observed that the stream lines becomes relatively straight in the center of the channel as compares to the walls of the channel and similar to (Chow et al., 1971).

The distribution of wall shear stress across the stenosis has been described for the variation of Re in figure 4(a) for fixed $\epsilon = 0.2$, $\delta = 0.1$. An increase in Re , wall shear stress increases near the throat of stenosed region and becomes negative in the converging and diverging section of channel

due to back flow. The adverse shearing in converging and diverging sections of channel indicates that there is point of separation in the upstream region and reattachment point in the downstream region of channel. It is observed that wall shear stress holds for both small and large Re .

In figure 4(b) effect of ϵ on wall shear stress is presented. The straight line indicates that there is no stenosis and the flow is Poiseuille flow. By the increase in ϵ wall shear stress increases over the stenosed region and becomes negative in the converging section of channel due to adverse flow, which is prediction for the point of separation. The separation point was considered to be the point nearest the throat where reversed flow along the wall of channel could be observed. The point farthest down stream from the throat where back flow occur is defined as reattachment point. It is expected that the wall shear stress plays an important role in the formation of the stenosis and its further growth. Because the deposit of cholesterol and proliferation of connective tissue may be responsible for the abnormal growth in lumen of artery. Its actual cause may not be known exactly but its effect on the cardiovascular system can easily be understood by studying the blood flow in its vicinity. One of the practical applications of blood flow through a membrane oxygenator is the flow with an irregular wall surface.

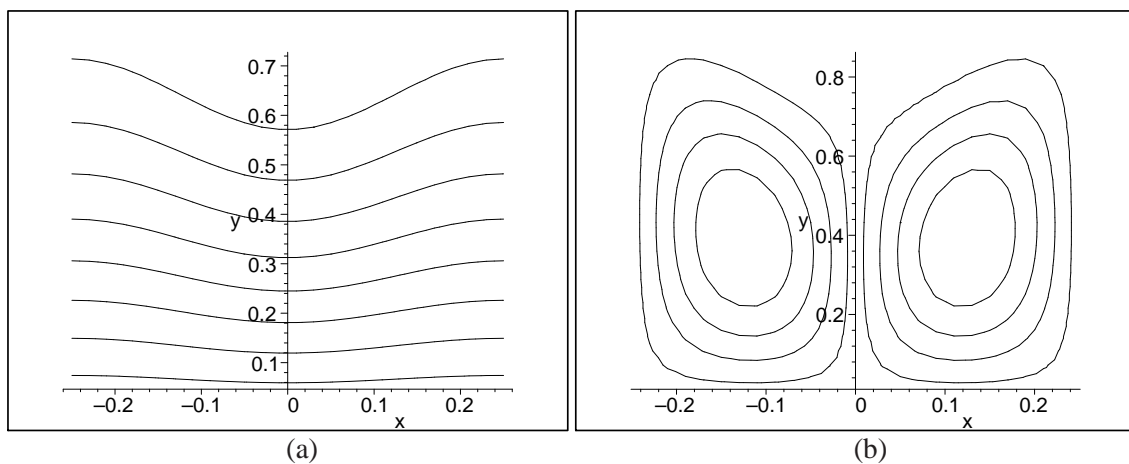


Figure 2. The zeroth order stream lines for $\epsilon = 0.20, Re = 12, \delta = 0.1$ are shown in (a) and the first order stream lines are shown in (b).

Figure 5(a) depict the distribution for the point of separation in converging section of channel for different ϵ along with fixed δ . The separation point lie to the right of minimum point, actually the purpose for zero wall shear stress is to find the critical Reynolds number where separation occur. The critical value of Re in the converging region for $\epsilon = 0.6$ is 70. The theory that the critical Re decreases with the increase in ϵ is verified. In figure 5(b) zero wall shear stress is plotted for ϵ having fixed value of δ in diverging section of channel. The aim of investigation is to determine the critical value of Re at which reattachment occurred in the diverging region of the channel. As the critical Re reached the reattachment occur in the diverging region of channel and separation point occur in the upstream region of channel. It is observed that the critical value of Re for $\epsilon = 0.6$ is 380. It is also observed form figure 6 that as ϵ increases critical value of Re decreases.

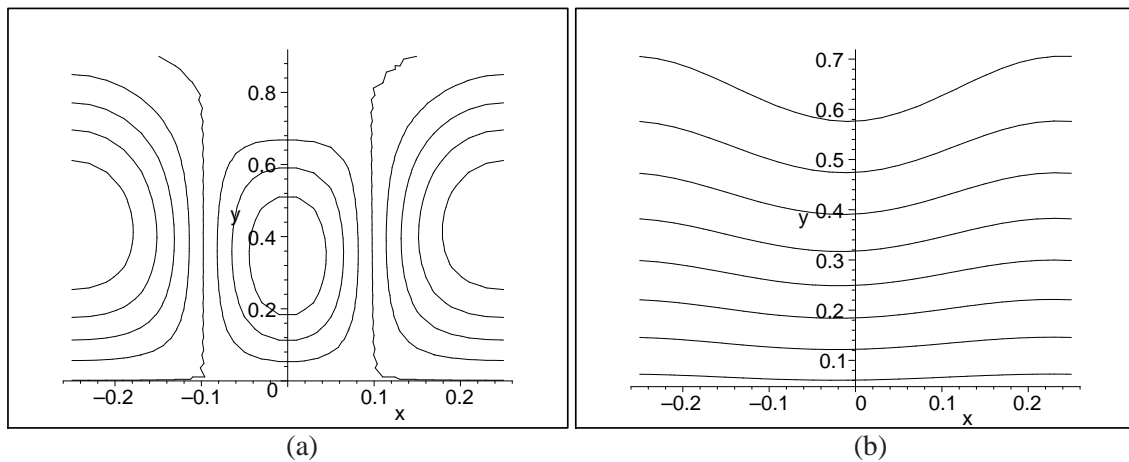


Figure 3. The second order stream lines are shown in (a) and the streamlines correct up to the second order in δ are shown in (b).

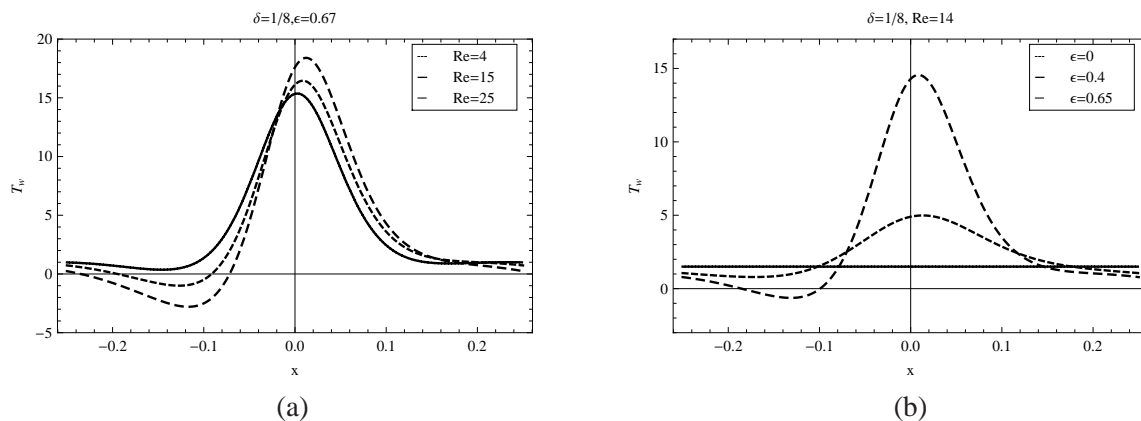


Figure 4. The effect of Re on wall shear stress is shown in (a) and the effect of ϵ on wall shear stress is shown in (b).

Figure 6(a) presents the effect for the various values of Re on pressure distribution. It may be noted that with the increase in Re leads to increase the pressure gradient over the stenosed region and becomes negative in the converging and diverging regions, due to the dependence of Re on average velocity. The adverse pressure gradient in these regions causes back flows as observed earlier. These back flows predicts the separation point in converging region and reattachment point in diverging region of the channel. It is observed that the magnitude of adverse pressure gradient in the diverging region is smaller as compared to that in the converging region.

Effect of ϵ on pressure gradient is studied in figure 6(b). It is observed that with the increase in ϵ , pressure gradient increases over the region having stenosis and becomes negative in the upstream and downstream regions of channel due to back flow. The adverse pressure gradient in the converging part of stenosis describing the flow separation and reattachment in the diverging

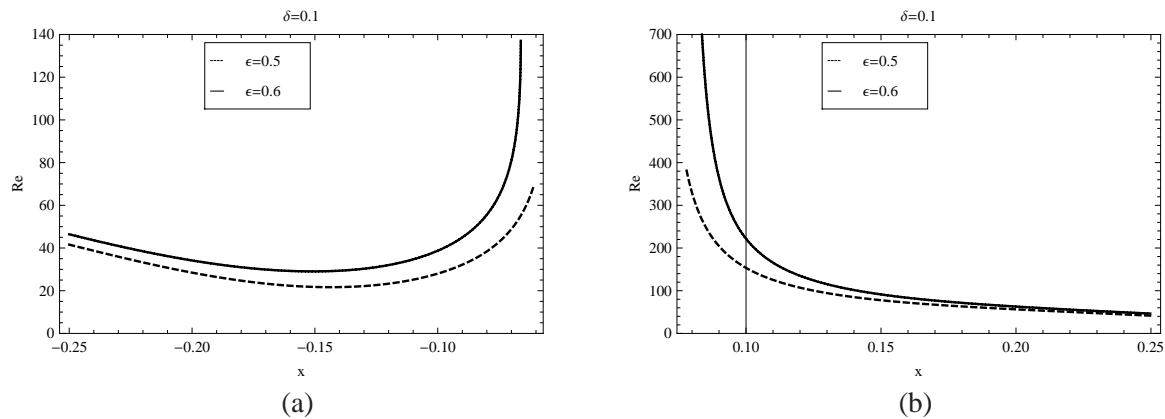


Figure 5. The separation point in converging region are shown in (a) and the reattachment point in diverging region are shown in (b).

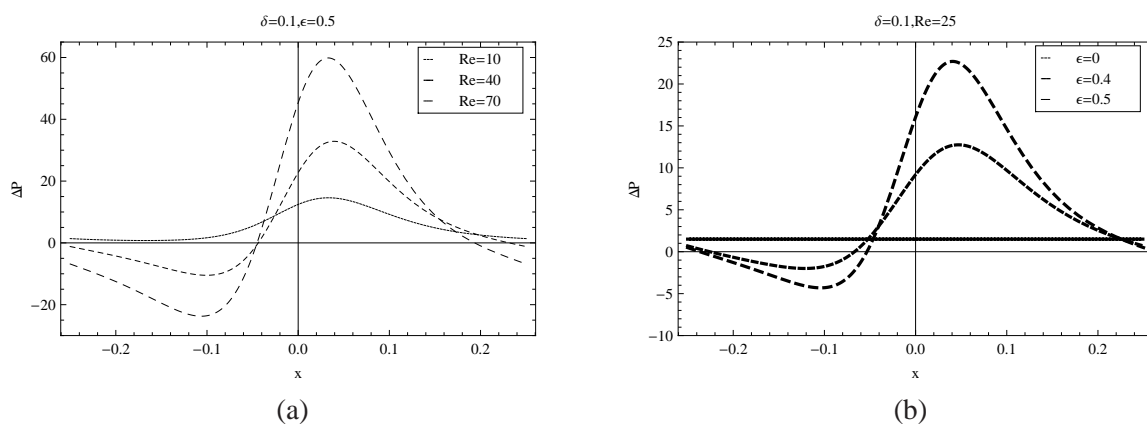


Figure 6. The pressure distribution for Re is shown in (a) and the pressure distribution for ϵ is shown in (b).

part. The straight line preserve Poiseuille flow as there is no stenosis.

Figure 7(a) depict for various values of Re on axial component of velocity. It is observed that with the increase in Re the axial velocity is maximum over the obstructive region and becomes negative causing back flow in the converging and diverging sections of the channel. Figure 7(b) shows the effect of ϵ on velocity distribution. It is observed that as the ϵ increases the velocity increases over the stenosed region and decreases sharply in the converging section and then recover it in the diverging section of channel. Negative velocity indicates the back flow, due to separation and reattachment points in the channel.

Figure 8(a) shows the effect of Pe on temperature distribution. It is observed that with the increase in Pe , temperature increases over the stenosed region and becomes negative in the converging and diverging regions. The adverse temperature in the upstream and downstream sections

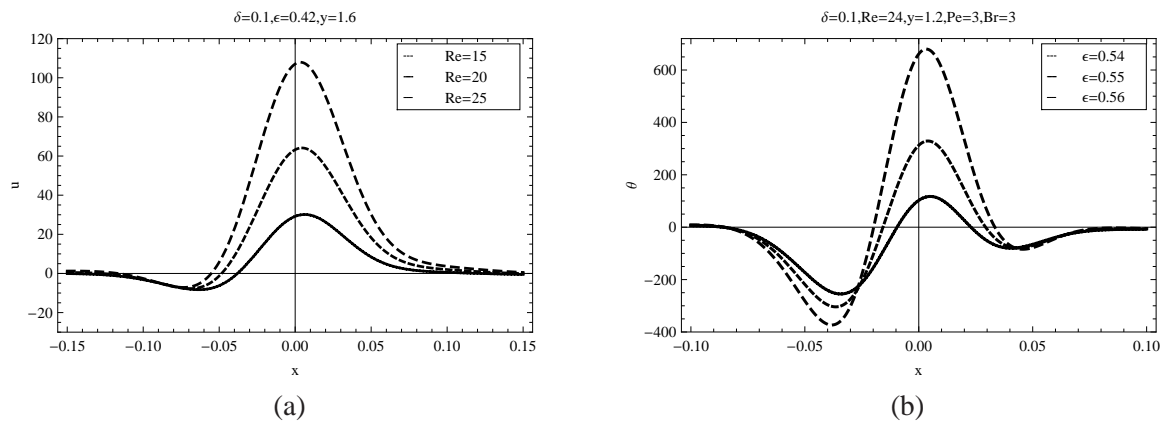


Figure 7. The axial velocity distribution for Re is shown in (a) and the axial velocity distribution for ϵ is shown in (b).

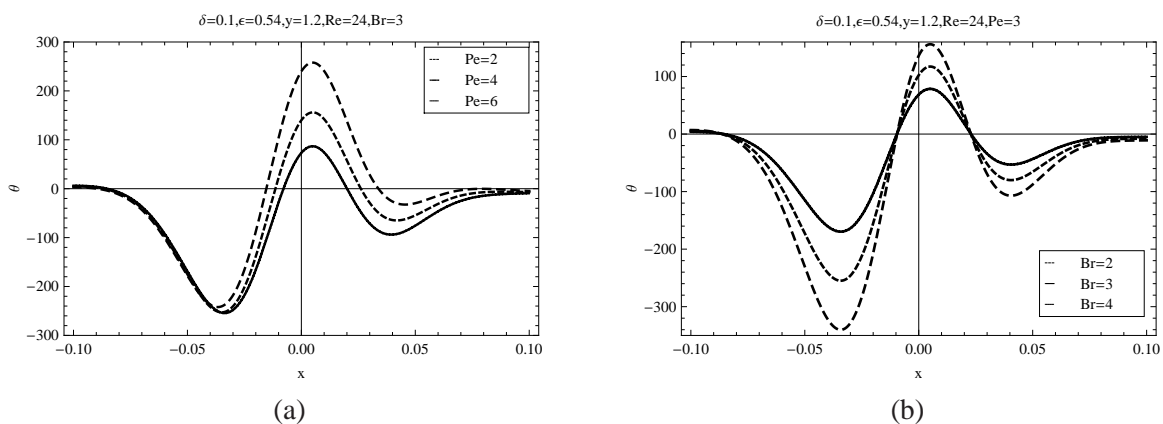


Figure 8. The effect of Pe on temperature distribution is shown in (a) and the effect of Br on temperature distribution is shown in (b).

describing flow separation and reattachment from the wall also confirm the results for velocity and wall shear stress. Temperature distribution across the stenosis has been described in figure 8(b) for different values of Br . Temperature increases steeply from its axial axis in the converging section of the stenosis to the peak value at the throat, then drop to a minimum value downstream behind the stenosis and again approaches to the axial axis in the region away from stenosis. The magnitude of adverse temperature in the diverging region of stenosis is smaller as compared to that in the converging section of the stenosis. The adverse temperature in these regions cause back flow as observed earlier in velocity and pressure fields.

7. Summary

In the present study, steady two-dimensional flow of incompressible Newtonian fluid with heat transfer between two parallel plates in the presence of a cosine shaped stenosis is presented. The underlying problem is solved with the help of the regular perturbation method. The results thus obtained are discussed graphically in terms of stream lines, pressure gradient, wall shear stress, separation and reattachment points and temperature distribution. It is observed that the general pattern of streamlines is similar as discussed in (Layek & Midya, 2007) - (Chow *et al.*, 1971), wall shear stress is same as given by (Morgan & Young, 1974) - (Haldar, 1991) and separation and reattachment points are in agreement with (Haldar, 1991). It is observed that:

- Stream lines for zeroth order and up to second order are similar due to small δ and first and second order shows rotational motion.
- Increase in Reynolds number increases the wall shear stress, velocity and pressure gradient.
- Increase in thickness of stenosis increases pressure gradient, temperature and wall shear stress causing separation and reattachment in the channel.
- Increase in the thickness of stenosis decreases the critical Reynolds number for separation and reattachment points, means even at low velocity separation occurs.
- By the increase in Peclet and Brinkman number increases the temperature between the channel.
- For $\epsilon = 0$ Poiseuille flow is recovered.

References

- Chakravarty, S. and A. G. Chakravarty (1988). Response of blood flow through an artery under stenotic conditions. *Rheologica Acta*.
- Chow, J. C. F., K. Soda and C. Dean (1971). On laminar flow in wavy channel. In: *Developments in Mechanics, Vol. 8, Proceedings of the 12th. Midwestern Mechanics Conference, University of Notre Dame Press, Notre Dame, Indiana*. pp. 247–260.
- Forrester, J. H. and D. F. Young (1970). Flow through a converging-diverging tube and its implications in occlusive vascular disease. *Journal of Biomechanics* **3**, 297–316.
- Haldar, K. (1985). Effect of the shape of stenosis on the resistance to blood flow through an artery. *Bulletin of Mathematical Biology* **47**, 545–550.
- Haldar, K. (1991). Analysis of separation of blood flow in constricted arteries. *Archives of Mechanics* **43**(1), 107–113.
- Kruszewski, A., R. Wang and T.M. Guerra (2008). Nonquadratic stabilization conditions for a class of uncertain nonlinear discrete time ts fuzzy models: A new approach. *IEEE Transactions on Automatic Control* **53**(2), 606–611.
- Layek, G. C and C. Midya (2007). Effect of constriction height on flow separation in a two-dimensional channel. *Communications in Nonlinear Science and Numerical Simulation* **12**, 745–759.
- Lee, J. S. and Y. C. Fung (1970). Flow in locally constricted tubes at low Reynolds number. *Journal of Applied Mechanics* **37**, 9–16.

- Mehrotra, R., G. Jayaraman and N. Padmanabhan (1985). Pulsatile blood flow in a stenosed artery - a theoretical model. *Medical Biological Engineering and Computing* **23**, 55–62.
- Morgan, B. E. and D. F. Young (1974). An integral method for the analysis of flow in arterial stenoses. *Bulletin of Mathematical Biology* **36**, 39–53.
- Newman, D. L., N. Westerhof and P. Sipkema (1979). Modelling of aortic stenosis. *Journal of Biomechanics* **12**, 229–235.
- Srivastava, V. P. and R. Rastogi (2010). Blood flow through a stenosed catheterized artery: Effects of hematocrit and stenosis shape. *Computers and Mathematics with Applications* **59**(4), 1377–1385.

Appendix 1

List of Mathematical Symbols

\mathbf{V}	Velocity vector (m/s)
∇	del operator
p	scalar pressure(Pa)
d/dt	material time derivative
c_p	specific heat(J/kgK)
T	temperature($^{\circ}$ C)
u, v	velocity components(m/s)
x, y	coordinate axis(m)
\mathbf{A}_1	first Rivlin-Ericksen tensor
$l_o/2$	length of stenosis(m)
$h(x)$	variable width between the stenosis(m)
h_o	radius of unobstructed channel(m)
u_o	average velocity(m/s)
Q	volume flow rate(m^3/s)
T_1, T_o	temperatures on boundary of stenosis and fluid($^{\circ}$ C)
Re	Reynolds number
Br	Brinkman number
Pe	Peclet number
$f(x)$	boundary profile
τ	extra stress tensor
ρ	density
κ	thermal conductivity
ϕ	viscous dissipation function
μ	dynamic viscosity(Pa/s)
\top	transpose
λ, ϵ	maximum height of stenosis
θ	dimensionless temperature
ν	kinematic viscosity(m^2/s)
ψ	stream function
δ	constant
η	ratio of y and f
τ_{ω}	wall shear stress